Available online at www.sciencedirect.com
ScienceDirect
Trans. Nonferrous Met. Soc. China 21(2011) 2454−2458

Transactions of
Nonferrous Metals
Society of China
www.tnmsc.cn

Influence of Li_3PO_4 addition on properties of lithium ion-conductive electrolyte $Li_{1.3}Al_{0.3}Ti_{1.7}(PO_4)_3$

XIAO Zhuo-bing [1], CHEN Shang[2], GUO Man-man[1]

1. Key Laboratory of Hunan Forest Products and Chemical Industry Engineering, Zhangjiajie 427000, China;
2. College of Chemistry and Chemical Engineering, Jishou University, Jishou 416000, China

Received 18 April 2010; accepted 19 September 2011

Abstract: The sintered $Li_{1.3}Al_{0.3}Ti_{1.7}(PO_4)_3$ pellets with different mole fractions of Li_3PO_4 were prepared by sol−gel method. The structure, surface morphology, electrochemical window, ionic conductivity and activation energy of the sintered pellets were studied by X-ray diffraction, scan electron microscopy, cyclic voltammetry, and electrochemical impedance spectroscopy. The results show that all the sintered $Li_{1.3}Al_{0.3}Ti_{1.7}(PO_4)_3$ pellets with different mole fractions of Li_3PO_4 have similar X-ray diffraction patterns. The sintered $Li_{1.3}Al_{0.3}Ti_{1.7}(PO_4)_3$ pellet with Li_3PO_4 shows a lower porosity and is denser than the one without Li_3PO_4. The addition of Li_3PO_4 has a large effect on the porosity and density of the sintered $Li_{1.3}Al_{0.3}Ti_{1.7}(PO_3)_4$ pellet, and little effect on its electrochemical window. Among the sintered $Li_{1.3}Al_{0.3}Ti_{1.7}(PO_3)_4$ pellets with different mole fractions of Li_3PO_4, the one with 1% Li_3PO_4 shows the activation energy of 0.314 2 eV and the highest ionic conductivity of 6.15×10^{-4} S/cm.

Key words: sol−gel; electrolyte; ionic conduction

---

1 Introduction

Lithium titanium phosphate, $LiTi_2(PO_4)_3$, which is based upon the NASICON (Na+super-ionic+conductor) framework with a space group of $R\bar{3}C$, has been studied as a lithium-ion-conductive solid electrolyte [1−2]. It is one of the promising lithium ion-conductive solid electrolytes. However, its conductivity is not high enough for practical applications [3−4]. In order to obtain $LiTi_2(PO_4)_3$ with a higher ionic conductivity, some researchers replaced Ti with Zr [2], Nb [5], La [6], Y [7], and Ge [8]. However, these studies did not result in satisfied ionic conductivity. AONO et al [9] reported that Al-doping was effective for the enhancement of lithium ion conduction. Since then, a lot of attention has been paid to $Li_{1.3}Al_{0.3}Ti_{1.7}(PO_4)_3$ for possible use in solid-state lithium-ion batteries [10−15].

Sol−gel method is one of the most frequently employed techniques to synthesize various materials. The technique has several advantages including good mixture of the reagents, relatively low crystallization temperature, homogenous and small grain size of product. The small grained powders can result in sintered pellet with high density, small voids and grains, which leads to a high ionic conductivity [16].

Flux can influence the sinterability and therefore affect the ionic conductivity and strength of the sintered electrolyte pellet [17]. Considering Li_3PO_4 a good flux with a relatively low melting temperature of 837 °C, the characterization of sol−gel derived $Li_{1.3}Al_{0.3}Ti_{1.7}(PO_4)_3$ with different mole fractions of Li_3PO_4 flux is studied in the present work to obtain $Li_{1.3}Al_{0.3}Ti_{1.7}(PO_4)_3$ pellet with high ionic conductivity and strength, which can be used in thin-film battery as both electrolyte and substrate. To the author’s knowledge, there are few reports about the influence of Li_3PO_4 addition on the properties of lithium ion-conductive electrolyte $Li_{1.3}Al_{0.3}Ti_{1.7}(PO_4)_3$.

2 Experimental

$Li(CH_3COO)\cdot2H_2O$ and $Al(NO_3)_3\cdot9H_2O$ at stoichiometric amount were dissolved in $CH_3OCH_2CH_2OH$. Then $PO(OC_4H_9)_4$ and $Ti(OC_4H_9)_4$ were consecutively dripped into the mixture under constant stirring to form $Li_{1.3}Al_{0.3}Ti_{1.7}(PO_4)_3$ precursor

---

Foundation item: Project supported by Aid Program for Science and Technology Innovative Research Team (Chemicals of Forestry Resources and Development of Forest Products) in Higher Educational Institutions of Hunan Province; Project (2009FJ3045) supported by the Fund of Science and Technology Department of Hunan Province, China

Corresponding author: XIAO Zhuo-bing; Tel: +86-744-8231386; E-mail: xiaoyddd@163.com

DOI: 10.1016/S1003-6326(11)61036-4

solution. Then several drops of deionized water were added into the solution followed by drying in an oven at 140 °C for 4 h to get $Li_{1.3}Al_{0.3}Ti_{1.7}(PO_4)_3$ gel. The gel was calcined at 900 °C for 2 h to obtain $Li_{1.3}Al_{0.3}Ti_{1.7}(PO_4)_3$ powders. The powders were mixed with different mole fractions of Li_3PO_4 and pressed into pellets at the pressure of 100 MPa using 3% polyvinyl-alcohol solution as the binder. The pressed pellets were calcined at 900 °C for 2 h to obtain $Li_{1.3}Al_{0.3}Ti_{1.7}(PO_4)_3$ pellets with different mole fractions of Li_3PO_4.

The structural identification of the sintered $Li_{1.3}Al_{0.3}Ti_{1.7}(PO_4)_3$ pellets with different mole fractions of Li_3PO_4 was conducted by X-ray diffraction. The surface morphology was studied by scan electron microscopy. The compositions of the synthesized powders were determined by the inductively coupled plasma (ICP) method. Porosity of the sintered pellets was determined by the Archimedes's method. For the measurement of electrochemical window, cyclic voltammetry was carried out using micro-electrode fabricated from grounded $Li_{1.3}Al_{0.3}Ti_{1.7}(PO_4)_3$ pellet. The micro-electrode was placed in an beaker cell containing 1 mol/L LiPF6 dissolved in ethylene and dimethyl carbonate (1:1, volumetric ratio). Metal lithium was used as both counter and reference electrodes. The ionic conductivity and activation energy were measured by electrochemical impedance spectroscopy. Both sides of the sintered pellet were painted with silver slurry followed by drying at 150 °C for 30 min before the electrochemical measurements were carried out. Electrochemical impedance measurement was conducted in an Ar-flowed tube over the frequency range of 1 Hz to 100 kHz at different temperatures.

3 Results and discussion

The X-ray diffraction patterns of the sintered $Li_{1.3}Al_{0.3}Ti_{1.7}(PO_4)_3$ pellets with different mole fractions of Li_3PO_4 are displayed in Fig. 1. As observed in Fig. 1, all the sintered pellets show similar diffraction patterns belonging to rhombohedral symmetry (space group $R\overline{3}C$) with six formula units in the unit cell. No diffraction peaks of impure phase are identified. All the diffraction peaks of the sintered pellets agree well with the reports for $Li_{1.3}Al_{0.3}Ti_{1.7}(PO_4)_3$ [11], suggesting that the sintered pellets are pure $Li_{1.3}Al_{0.3}Ti_{1.7}(PO_4)_3$ phase. There are no obviously difference in the lattice parameters between $Li_{1.3}Al_{0.3}Ti_{1.7}(PO_4)_3$ pellets with and without Li_3PO_4, indicating that the addition of Li_3PO_4 flux has little effect on the crystal structure of $Li_{1.3}Al_{0.3}Ti_{1.7}(PO_4)_3$.

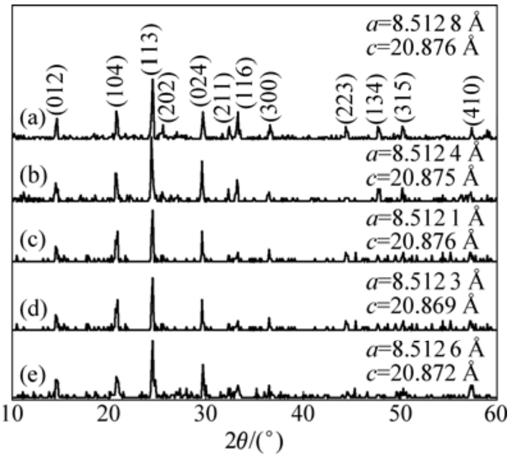

Fig. 1 XRD patterns and lattice parameters of sintered $Li_{1.3}Al_{0.3}Ti_{1.7}(PO_4)_3$ pellets with different mole fractions of Li_3PO_4: (a) 0; (b) 1%; (c) 2%; (d) 3%; (e) 4%

The scan electron micrographs of the sintered $Li_{1.3}Al_{0.3}Ti_{1.7}(PO_4)_3$ pellets with different mole fractions of Li_3PO_4 are presented in Fig. 2. As seen in Fig. 2, the contact between the particles of the sintered $Li_{1.3}Al_{0.3}Ti_{1.7}(PO_4)_3$ pellets with Li_3PO_4 flux is better than the one without Li_3PO_4, which can be attributed to the relatively low melting temperature of Li_3PO_4, namely, Li_3PO_4 can melt and fill the space between $Li_{1.3}Al_{0.3}Ti_{1.7}(PO_4)_3$ particles during the sintering at 900 °C, leading to better sinterability and densification. However, there are no obvious differences between the sintered pellets with Li_3PO_4.

The porosity of sintered $Li_{1.3}Al_{0.3}Ti_{1.7}(PO_4)_3$ pellets with different mole fractions of Li_3PO_4 is displayed in Fig. 3. As shown in Fig. 3, the porosity of sintered $Li_{1.3}Al_{0.3}Ti_{1.7}(PO_3)_4$ pellets with 1%, 2%, 3%, and 4% Li_3PO_4 are 2.45%, 2.38%, 2.17%, and 2.15%, respectively, which are lower than 3.78% for the one without Li_3PO_4. The reason why the sintered $Li_{1.3}Al_{0.3}Ti_{1.7}(PO_4)_3$ pellets with Li_3PO_4 shows lower porosity than the one without Li_3PO_4 is that Li_3PO_4 melts and fills the space between $Li_{1.3}Al_{0.3}Ti_{1.7}(PO_4)_3$ particles during the sintering at 900 °C, resulting in the pellets with better sinterability and densification.

Electrochemical window of electrolyte is an important factor for its practical application, especially in the field of batteries. Figure 4 shows the redox voltages of the sintered pellet with different mole fractions of Li_3PO_4. As seen in Fig. 4, there are no significant differences between these sintered pellets. All the pellets show the redox voltage beyond 2.4 V. This indicates that the addition of Li_3PO_4 has little effect on the electrochemical window of $Li_{1.3}Al_{0.3}Ti_{1.7}(PO_4)_3$.

Electrochemical impedance spectra of the sintered $Li_{1.3}Al_{0.3}Ti_{1.7}(PO_3)_4$ pellets with different mole fractions of Li_3PO_4 conducted at 25 °C are shown in Fig. 5. All the sintered pellets show an incomplete semicircle and an inclined line. The incomplete semicircle in the spectrum is caused by the insufficient frequency upper limit of

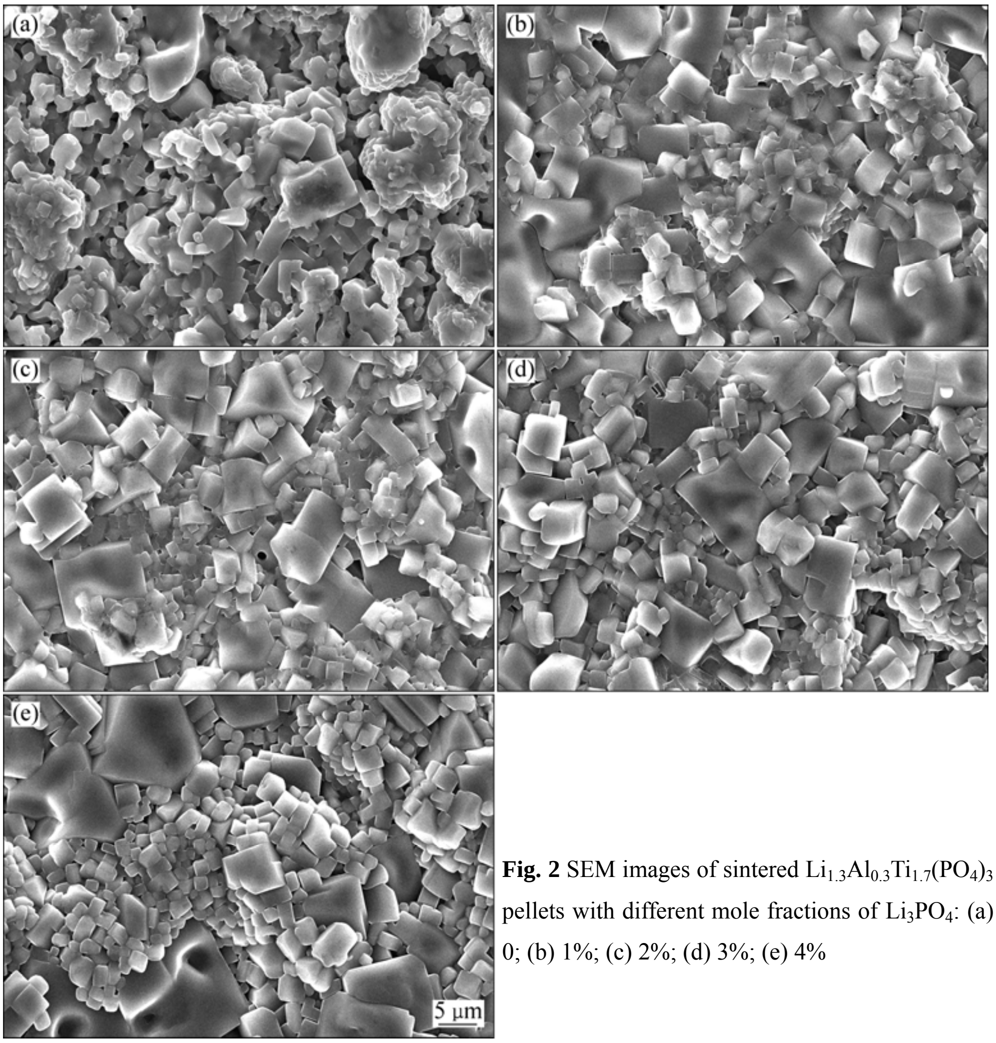

Fig. 2 SEM images of sintered $Li_{1.3}Al_{0.3}Ti_{1.7}(PO_4)_3$ pellets with different mole fractions of Li_3PO_4: (a) 0; (b) 1%; (c) 2%; (d) 3%; (e) 4%

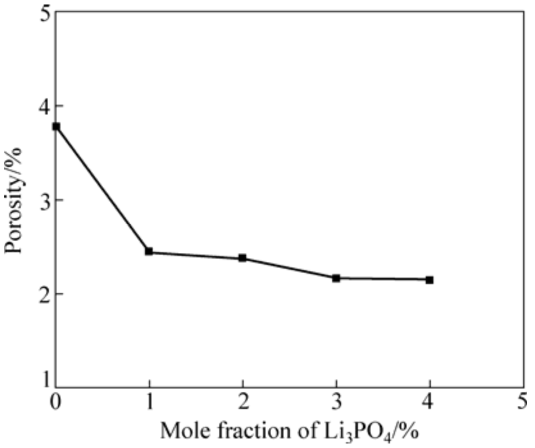

Fig. 3 Effect of mole fraction of Li_3PO_4 on porosity of sintered $Li_{1.3}Al_{0.3}Ti_{1.7}(PO_4)_3$ pellets

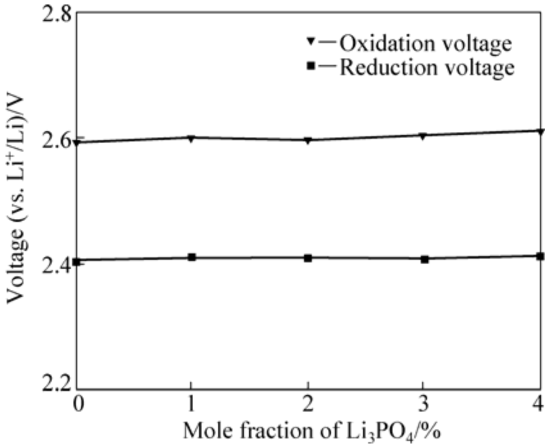

Fig. 4 Redox voltages of sintered $Li_{1.3}Al_{0.3}Ti_{1.7}(PO_4)_3$ pellets with different mole fractions of Li_3PO_4

electrochemical workstation CHI660B. The high-frequency limit should be more than 1 MHz because the time constant of the bulk process is 1 ns assuming a geometric capacity (c_{geo}) of 1−10 pF. Obviously, the high-frequency limit in this study of 100 kHz is insufficient and causes the incomplete semicircle, which makes it difficult to determine the bulk ionic conductivity. However, from the intercept of the inclined line in the diagram the total ionic conductivity of the sintered pellets with different mole fractions of Li_3PO_4 can be calculated.

Temperature dependence of ionic conductivity for

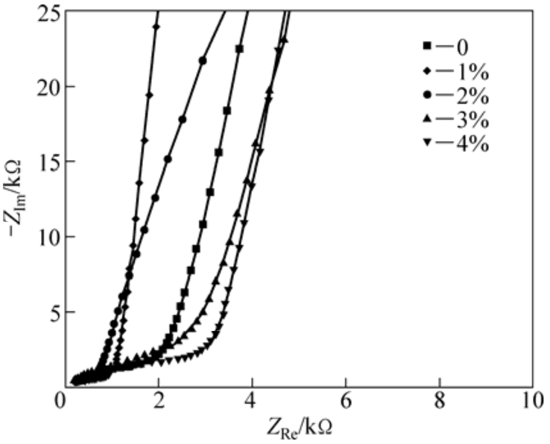

Fig. 5 Electrochemical impedance spectra of sintered $Li_{1.3}Al_{0.3}Ti_{1.7}(PO_4)_3$ pellets with different mole fractions of Li_3PO_4 conducted at 25 °C

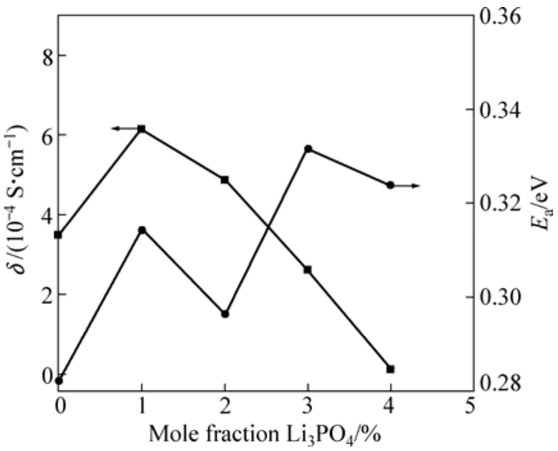

Fig. 7 Ionic conductivity and activation energies of sintered $Li_{1.3}Al_{0.3}Ti_{1.7}(PO_4)_3$ pellets with different mole fractions of Li_3PO_4 conducted at 25 °C

the sintered $Li_{1.3}Al_{0.3}Ti_{1.7}(PO_3)_4$ pellets with different mole fractions of Li_3PO_4 is presented in Fig. 6. All the sintered pellets result in a linear temperature-dependence of conductivity followed on Arrhinus's law. According to the results in the figure, the activation energy E_a can be obtained from the following equation:

$$\sigma = \sigma_0 \exp\left(\frac{-E_a}{RT}\right)$$

where σ_0 is the pre-exponential factor; E_a is the activation energy for conductor; R is the mole gas constant; and T is the thermodynamic temperature.

The ionic conductivity and activation energies of sintered $Li_{1.3}Al_{0.3}Ti_{1.7}(PO_4)_3$ pellets with different mole fractions of Li_3PO_4 are displayed in Fig. 7. As shown in Fig. 7, the ionic conductivities of the sintered $Li_{1.3}Al_{0.3}Ti_{1.7}(PO_4)_3$ with 1% and 2% Li_3PO_4 are higher than the one without Li_3PO_4. When the mole fraction of Li_3PO_4 increases from 0 to 1%, the ionic conductivity increases from 3.46×10^{-4} S/cm to 6.15×10^{-3} S/cm. However, the ionic conductivity decreases with further increase of Li_3PO_4. This effect of Li_3PO_4 addition on the ionic conductivity of $Li_{1.3}Al_{0.3}Ti_{1.7}(PO_4)_3$ may be caused by the following reasons: The increase of Li_3PO_4 leads to the pellet with better sinterability and densification because Li_3PO_4 is a good flux, which results in closer contact of $Li_{1.3}Al_{0.3}Ti_{1.7}(PO_4)_3$ particles and decreases the resistance at grain boundaries, leading to higher ionic conductivity. However, too much Li_3PO_4 addition also decreases the ionic conductivity of $Li_{1.3}Al_{0.3}Ti_{1.7}(PO_4)_3$ because the ionic conductivity of Li_3PO_4 is considerably lower than $Li_{1.3}Al_{0.3}Ti_{1.7}(PO_4)_3$. Figure 7 also shows the activation energies of sintered $Li_{1.3}Al_{0.3}Ti_{1.7}(PO_3)_4$ pellets with 0, 1%, 2%, 3%, and 4% Li_3PO_4 are 0.282 1, 0.314 2, 0.296 3, 0.331 5, and 0.323 7 eV, respectively. The activation energy of sintered $Li_{1.3}Al_{0.3}Ti_{1.7}(PO_3)_4$ with Li_3PO_4 is slightly higher than the one without Li_3PO_4. This means that the temperature has greater influence on the ionic conductivity of the sintered $Li_{1.3}Al_{0.3}Ti_{1.7}(PO_3)_4$ pellets with Li_3PO_4.

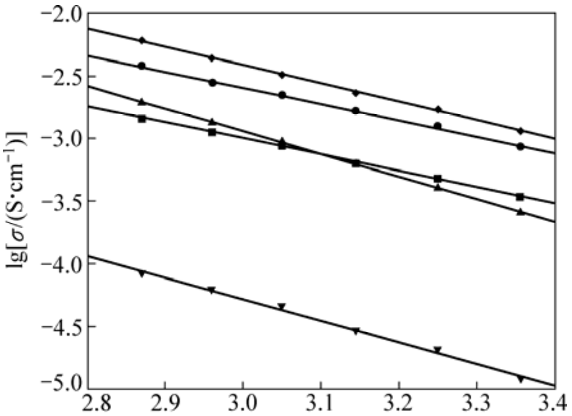

Fig. 6 Temperature dependence of conductivity for sintered $Li_{1.3}Al_{0.3}Ti_{1.7}(PO_3)_4$ pellets with different mole fractions of Li_3PO_4

4 Conclusions

1) The sintered $Li_{1.3}Al_{0.3}Ti_{1.7}(PO_4)_3$ pellets with different mole fractions of Li_3PO_4 show similar X-ray diffraction patterns. The sintered $Li_{1.3}Al_{0.3}Ti_{1.7}(PO_4)_3$ pellets with Li_3PO_4 show lower porosity and are denser than the one without Li_3PO_4.

2) The addition of Li_3PO_4 has little effect on the redox voltages of $Li_{1.3}Al_{0.3}Ti_{1.7}(PO_4)_3$. When the Li_3PO_4 addition increases from 0 to 1%, the ionic conductivity increases from 3.46×10^{-4} S/cm to 3.95×10^{-4} S/cm. However, the ionic conductivity decreases with further increase of Li_3PO_4.

3) The activation energies of sintered

$Li_{1.3}Al_{0.3}Ti_{1.7}(PO_3)_4$ pellets with 0, 1%, 2%, 3%, and 4% are 0.282 1, 0.246 9, 0.297 1, 0.327 3, and 0.341 9 eV, respectively. The activation of the sintered $Li_{1.3}Al_{0.3}Ti_{1.7}(PO_3)_4$ pellet with Li_3PO_4 is slightly higher than the one without Li_3PO_4.

References

[1] CHEN L J, ZHAO Y J, LUO J Y, XIA Y Y. Oxygen vacancy in $LiTiPO_5$ and $LiTi_2(PO_4)_3$: A first-principles study [J]. Phys Lett A, 2011, 375: 934−938.

[2] ARBI K, ROJO J M, SANZ J. Lithium mobility in titanium based NASICON $Li_{1+x}Ti_{2-x}Al_x(PO_4)_3$ and $LiTi_{2-x}Zr_x(PO_4)_3$ materials followed by NMR and impedance spectroscopy [J]. J Eur Ceram Soc, 2007, 27: 4215−4218.

[3] LUO J Y, CHEN L J, ZHAO Y J, HE P, XIA Y Y. The effect of oxygen vacancies on the structure and electrochemistry of $LiTi_2(PO_4)_3$ for lithium-ion batteries: A combined experimental and theoretical study [J]. J Power Sources, 2009, 194: 1075−1080.

[4] WOLFENSTINE J, ALLEN J L, SUMNER J, SAKAMOTO J. Electrical and mechanical properties of hot-pressed versus sintered $LiTi_2(PO_4)_3$ [J]. Solid State Ionics, 2009, 180: 961−967.

[5] VINOTH RATHAN S, GOVINDARAJ G. Thermal and electrical relaxation studies in $Li_{(4+x)}Ti_xNb_{1-x}P_3O_{12}$ ($0.0 \le x \le 1.0$) phosphate glasses [J]. Solid State Sciences, 2010, 12: 730−735.

[6] KAZAKEVIČIUS E, ŠALKUS T, DINDUNE A, KANEPE Z, RONIS J, KEŽIONIS A, KAZLAUSKIENĖ V, MIŠKINIS J, SELSKIENĖ A, SELSKIS A. La-doped $LiTi_2(PO_4)_3$ ceramics [J]. Solid State Ionics, 2008, 179: 51−56.

[7] ŠALKUS T, KAZAKEVIČIUS E, KEŽIONIS A, KAZLAUSKIENĖ V, MIŠKINIS J, DINDUNE A, KANEPE Z, RONIS J, DUDEK M, BUĆKO M. XPS and ionic conductivity studies on $Li_{1.3}Al_{0.15}Y_{0.15}Ti_{1.7}(PO_4)_3$ ceramics [J]. Ionics, 2010, 16: 631−637.

[8] XU X, WEN Z, GU Z, XU X, LIN Z, Lithium ion conductive glass ceramics in the system $Li_{1.4}Al_{0.4}(Ge_{1-x}Ti_x)_{1.6}(PO_4)_3$ (x=0–1.0) [J]. Solid State Ionics, 2004, 171: 207−213.

[9] AONO H, SUGIMOTO E, SADAOKA Y, IMANAKA N, ADACH G. Conductivity of the lithium titanium phosphate ($Li_{1+x}M_xTi_{2-x}(PO_4)_3$, M=Al, Sc, Y, and La) system [J]. J Electrochem Soc, 1989, 136: 590−591.

[10] XU X X, WEN Z Y, YANG X L, CHEN L D. Dense nanostructured solid electrolyte with high Li-ion conductivity by spark plasma sintering technique [J]. Materials Research Bulletin, 2008, 43: 2334−2341.

[11] BEST A S, FORSYTH M, MACFARLANE D R. Stoichiometric changes in lithium conducting materials based on $Li_{1+x}Al_xTi_{2-x}(PO_4)_3$: Impedance, X-ray and NMR studies [J].Solid State Ionics, 2000, 136−137: 339−344.

[12] WANG Y J, PAN Y, KIM D. Conductivity studies on ceramic $Li_{1.3}Al_{0.3}Ti_{1.7}(PO_4)_3$-filled PEO-based solid composite polymer electrolytes [J]. J Power Sources, 2006, 159: 690−701.

[13] WU X M, LI X H, ZHANG Y H, XU M F, HE Z Q. Synthesis of $Li_{1.3}Al_{0.3}Ti_{1.7}(PO_4)_3$ by sol-gel technique [J]. Mater Lett, 2004, 58: 1227−1230.

[14] PANG M, SUZUKI R, SAITO M, MACHIDA K, HANAWA H, NOJIRI Y, TANASE S. Fabrication and crystal line patterning of $Li_{1.3}Al_{0.3}Ti_{1.7}(PO_4)_3$ ion conductive glass by Ni atom heat processing method [J]. Appl Phys Lett, 2008, 92: 041112-1−3.

[15] KOSOVA N V, DEVYATKINA E T, STEPANOV A P, BUZLUKOV A L. Lithium conductivity and lithium diffusion in NASICON-type $Li_{1+x}Ti_{2-x}Al_x(PO_4)_3$ (x=0; 0.3) prepared by mechanical activation[J]. Ionics, 2008, 14: 303−311.

[16] BROUSSE T, FRAGNAUD P, MARCHAND R, SCHLEICH D M, BOHNKE O, WEST K. All oxide solid-state lithium-ion cells [J]. J Power Sources, 1997, 68: 412−415.

[17] AONO H, SUGIMOTO E, SADAOKA Y, IMANAKA N, ADACHI G. Ionic conductivity of $LiTi_2(PO_4)_3$ mixed with lithium salts [J]. Chem Lett, 1990, 190: 331−334.

添加剂 Li_3PO_4 对锂离子固体电解质 $Li_{1.3}Al_{0.3}Ti_{1.7}(PO_4)_3$ 性能的影响

肖卓炳[1]，陈 上[2]，郭满满[1]

1. 林产化工工程湖南省重点实验室，张家界 427000；
2. 吉首大学 化学化工学院，吉首 416000

摘 要：采用溶胶−凝胶法，添加不同比例的 Li_3PO_4 助熔剂，合成 $Li_{1.3}Al_{0.3}Ti_{1.7}(PO_4)_3$ 锂离子固体电解质烧结片，采用 X 射线衍射、扫描电子显微镜研究合成产物的结构与形貌，采用循环伏安及交流阻抗技术研究添加不同摩尔分数的 $Li_{1.3}Al_{0.3}Ti_{1.7}(PO_4)_3$ 固体电解质烧结片的结构、氧化−还原电位、离子电导率和活化能。结果表明：添加与未添加 Li_3PO_4 助熔剂的 $Li_{1.3}Al_{0.3}Ti_{1.7}(PO_4)_3$ 烧结片具有相似的 X 射线衍射结果。添加 Li_3PO_4 的 $Li_{1.3}Al_{0.3}Ti_{1.7}(PO_4)_3$ 烧结片的空隙率较小，更为致密。添加 Li_3PO_4 对 $Li_{1.3}Al_{0.3}Ti_{1.7}(PO_4)_3$ 的氧化−还原电位影响不大。在所有添加 Li_3PO_4 助熔剂的 $Li_{1.3}Al_{0.3}Ti_{1.7}(PO_4)_3$ 烧结片中，添加 1%(摩尔分数)Li_3PO_4 的烧结片具有最高的离子电导率 6.15×10^{-4} S/cm 和最低的活化能 0.314 2 eV。

关键词：溶胶−凝胶；电解质；离子电导

(Edited by YANG Hua)